Quarrier, C.L., et al., 2023, Pre-agricultural soil erosion rates in the midwestern United States: Geology, https://doi.org/10.1130/G50667.1

SUPPLEMENTAL MATERIAL

Pre-agricultural soil erosion rates in the midwestern U.S.

Caroline L. Quarrier, Jeffrey S. Kwang, Brendon J. Quirk, Evan A. Thaler, and Isaac J. Larsen

This file contains:

Supplementary text describing methods
Supplementary figures
Supplementary tables

^{10}Be Sample Preparation and Analysis

Samples from depth increments selected to capture the exponential ^{10}Be production profile were split and sub-samples were sieved to isolate 250–850 μm grains (Kohl and Nishiizumi, 1992). The 250-850 μm grain-size fraction was pre-treated by leaching with hot, dilute HCl followed by leaching in a heated solution of NaOH and H_2O_2. Pure quartz separates were generated by multiple, week-long etches in a heated ultrasonic bath using 2% HF (Kohl and Nishiizumi, 1992). Quartz purity was assessed by ICP-OES measurement of Al, K, Ca, Mg, Ti, and Fe. Following addition of ~250 μg of Be carrier, quartz was dissolved and Be was chemically separated at the University of Massachusetts Cosmogenic Nuclide Laboratory. Most ^{10}Be/^{9}Be ratios were measured at the Purdue Rare Isotope Measurement Laboratory, though some were analyzed at the Center for Accelerator Mass Spectrometry at Lawrence Livermore National Laboratory (Table S1).

The measured nuclide concentrations (N) reflect inherited ^{10}Be from prior exposure ($N_{t=0}$), duration of exposure (t), and denudation rate (ε). We used the Monte Carlo method of Hidy et al. (2010) to determine the contributions of inheritance, exposure duration, and denudation rate on the measured ^{10}Be concentration depth profiles:

$$N_{z,\varepsilon,t} = N_{t=0}e^{-\lambda t} + \frac{P_{z=0}}{\lambda + \varepsilon\rho_z/\Lambda}\, e^{-z\rho_z/\Lambda} \cdot (1 - e^{-(\lambda + \varepsilon\rho_z/\Lambda)t}), \qquad \text{(S1)}$$

where $P_{z=0}$ is the surface ^{10}Be production rate (atom g^{-1} yr^{-1}), λ is the ^{10}Be decay constant (4.997 x 10^{-7} yr^{-1}; Chmeleff et al., 2010), ρ_z is the depth-varying bulk density (g cm^{-3}), z is depth (cm), and Λ is the apparent attenuation length (g cm^{-2}). Equation S1 is solved by incorporating ^{10}Be production by nucleons using a reference spallation production rate, which we determined for each site using Lal (1991)/Stone (2000) scaling and a sea-level, high latitude ^{10}Be production

rate of 4.01 from Borchers et al. (2015). The Hidy *et al.* (2010) method also calculates muonic production based on a specified elevation and profile depth. We used a composite depth-dependent bulk density model based on measurements from all sites and an uncertainty of 20% (Figure S3, Table S5). Many of our bulk density samples were dry when weighed; to correct for this we assumed an additional 10 weight percent saturation of dried samples, based on the water content of moist bulk density samples.

Exposure age, inheritance, and denudation rate are treated as unknowns in the Hidy et al. (2010) method, but the range of solutions can be constrained based on independent data. Hence, we set the upper and lower bounds on exposure age using published deglaciation chronologies for each site (Table S2). Erosion rate and erosion threshold parameters are set to have minimum values of 0 cm ka^{-1} and 0 cm, respectively, and maximum values that are sufficiently high that they do not restrict possible solutions. We ran 100,000 Monte Carlo simulations for each site to obtain the most probable values for inheritance, exposure age, and denudation rate. We use the Bayesian most probable results for exposure age and inheritance concentration since the Bayesian results more accurately represent the most probable solutions than do the mode results. For denudation rates, however, we use the mode because the Bayesian most probable denudation rate for Bernau and Kurtz is zero, which is incompatible with the non-zero chemical denudation indicated by geochemical mass balance at those sites.

For Hayden, a site for which glacial chronology is not well constrained, we ran simulations with two alternate maximum exposure ages: 677 ka, i.e., MIS 16 (Batchelor et al., 2019), and 2.7 Ma, i.e., the latter which is a conservative estimate that slightly pre-dates the oldest documented Pleistocene glaciation in the region (Balco et al., 2005; Balco and Rovey, 2010; Kerr et al., 2021). Both analyses yield a mode denudation rate of 0.059 mm yr^{-1}. Results from both simulations are included in the supplemental tables, and results reported in main text figures are those with a maximum age of 677 ka.

For sites where bioturbation homogenized surface ^{10}Be concentrations, we only used samples from below the depth of bioturbation to fit the depth profile (Figure S2). At Willis, samples between those at the surface and 270 cm depth yielded insufficient quartz for ^{10}Be measurement. Hence for that site we shifted the surface sample concentration to a depth of 36 cm, i.e., near the base of the bioturbation zone observed in profiles at other sites, to obtain a profile that more accurately reflects the relationship between concentration and depth.

XRF Sample Preparation and Analysis

The ^{10}Be-derived denudation rate quantifies the combined mass loss due to physical erosion and chemical weathering:

$$\varepsilon = E + W, \qquad \text{(S2)}$$

where ε is the denudation rate, E is the physical erosion rate, and W is the chemical weathering rate (Riebe et al., 2003). Here we use ε to represent the denudation rate, rather than the more commonly used notation D, as we use D in the main text to refer to the topographic diffusion coefficient.

To directly compare our measurements against previously measured agricultural erosion rates in the adjacent fields, we partitioned the total denudation rates we measured using ^{10}Be into physical erosion rate and chemical denudation rate components. Because chemical weathering removes mobile elements, it causes the progressive enrichment of chemically immobile elements within weathered soil (Riebe et al., 2003). By comparing the concentrations of an immobile element, Zr, in weathered soil and unweathered parent material, we calculated the chemical depletion fraction (CDF), or the percentage of denudation caused by chemical weathering, as follows:

$$CDF = 1 - ([Zr]_{parent}/[Zr]_{soil}), \quad \text{(S3)}$$

where $[Zr]_{parent}$ and $[Zr]_{soil}$ are the concentrations of Zr in the parent material and soil, respectively (Riebe et al., 2003). We calculated a CDF for each site using the uppermost and lowermost samples from each depth profile as the *soil* and *parent* terms, respectively (Table S4). We then calculated the proportion of denudation caused by physical erosion and, thus, soil erosion rates. The CDF is equal to W / ε, hence:

$$W = \varepsilon \cdot (1 - [Zr]_{parent}/[Zr]_{soil}), \quad \text{(S4)}$$

and by substituting the solution to eq. S4 into eq. S2 to solve for E, values of ε, W, and E were determined for each study site.

We measured the concentrations of major and trace elements in prairie depth profiles via X-ray fluorescence (XRF) (Tables S6 and S7). Dried samples were gently crushed with a mortar and pestle to break up aggregates, sieved to remove the >2 mm fraction, ground to a fine powder using a tungsten carbide ring mill, then pressed into pellets or fused for trace and major element analysis, respectively. Samples were analyzed in the Ronald B. Gilmore X-Ray Fluorescence Laboratory at the University of Massachusetts.

Estimation of the Diffusion Coefficient

The diffusion coefficient (m^2/yr) is found by relating erosion rate (m/yr) and topographic curvature (m^{-1}). As landscape erodes via diffusive processes, the curvature of the landscape decreases. Since present-day curvature values are lower than curvature values have been in the time following deglaciation, the diffusion coefficient we calculate overestimated. We calculate the degree of overestimation using an equation modified from Thaler et al. (2022). The true estimate of the diffusion coefficient, D, can be determined by the following implicit equation:

$$D_{estimate} = \frac{1-e^{-\frac{D\pi^2}{L_h^2}t}}{t\frac{\pi^2}{L_h^2}e^{-\frac{D\pi^2}{L_h^2}t}} \quad \text{(S5)}$$

where $D_{estimate}$ is the overestimated value of the diffusion coefficient (m^2/yr), L_h is a hillslope length, D is the corrected diffusion coefficient (m^2/yr), and t is the duration of erosion (yr). A typical hillslope length at the study sites is 63 m (Thaler et al., 2022). For the Des Moines lobe sites, the landform age (t) ranges from 13,500 to 21,100 yr. Assuming $D_{estimate}$ is 0.005 m^2/yr, the corrected value of D is 0.0046 m^2/yr for 13,500 yr of exposure and is 0.0044 for 21,000 years of exposure. Therefore, our estimate is assumed to be overestimated by approximately 10%. Since D is overestimated, the value of 0.005 m^2/yr is a conservative estimate, because the difference between the pre-agricultural and agricultural diffusion coefficients is greater than we estimate.

REFERENCES CITED

Balco, G., Rovey, C.W. II, 2010, Absolute chronology for major Pleistocene advances of the Laurentide ice sheet. Geology, v. 38. P. 795-798. doi.org/10.1130/G30946.1

Balco, G., Rovey, C.W. II, and Stone, J.O.H., 2005, The first glacial maximum in North America. Science, v. 307, p. 222. doi.org/10.1126/science.1103406

Borchers, B., Marrero, S., Balco, G., Caffee, M., Goehring, B., Lifton, N., Nishiizumi, K., Phillips, F., Schaefer, J., and Stone, J., 2016, Geological calibration of spallation production rates in the CRONUS-Earth project: Quaternary Geochronology, v. 31, p. 188-198, doi: 10.1016/j.quageo.2015.01.009.

Chmeleff, J., von Blanckenburg, F., Kossert, K. and Jakob, D., 2010, Determination of the ^{10}Be half-life by multicollector ICP-MS and liquid scintillation counting: Nuclear Instruments and Methods in Physics Research Section B: Beam Interactions with Materials and Atoms, v. 268, no. 2, p.192-199, doi: 10.1016/j.nimb.2009.09.012.

Hidy, A.J., Gosse, J.C., Pederson, J.L., Mattern, J.P., and Finkel, R.C., 2010, A geologically constrained Monte Carlo approach to modeling exposure ages from profiles of cosmogenic nuclides: an example from Lees Ferry, Arizona: Geochemistry Geophysics Geosystems, n. 11, Q0AA10, doi:10.1029/2010GC003084.

Kerr, P.J., Tassier-Surine, S.A., Kilgore, S.M., Bettis III, E.A., Dorale, J.A., and Cramer, B.D., 2021, Timing, provenance, and implications of two MIS 3 advances of the Laurentide Ice Sheet into the Upper Mississippi River Basin, USA: Quaternary Science Reviews, v. 261, 106926, doi: 10.1016/j.quascirev.2021.106926.

Kohl, C.P., and Nishiizumi, K., 1992, Chemical isolation of quartz for measurement of in-situ-produced cosmogenic nuclides: Geochimica et Cosmochimica Acta, v. 56, p. 3583-3587.

Lal, D., 1991, Cosmic ray labeling of erosion surfaces: in situ nuclide production rates and erosion models: Earth and Planetary Science Letters, v. 104, p. 424-439.

Riebe, C.S., Kirchner, J.W., and Finkel, R.C., 2003, Long-term rates of chemical weathering and physical erosion from cosmogenic nuclides and geochemical mass balance: Geochimica et Cosmochimica Acta, v. 67, no. 22, p. 4411-4427.

Stone, J., 2000, Air pressure and cosmogenic isotope production: Journal of Geophysical Research, v. 105, p. 23753–23760.

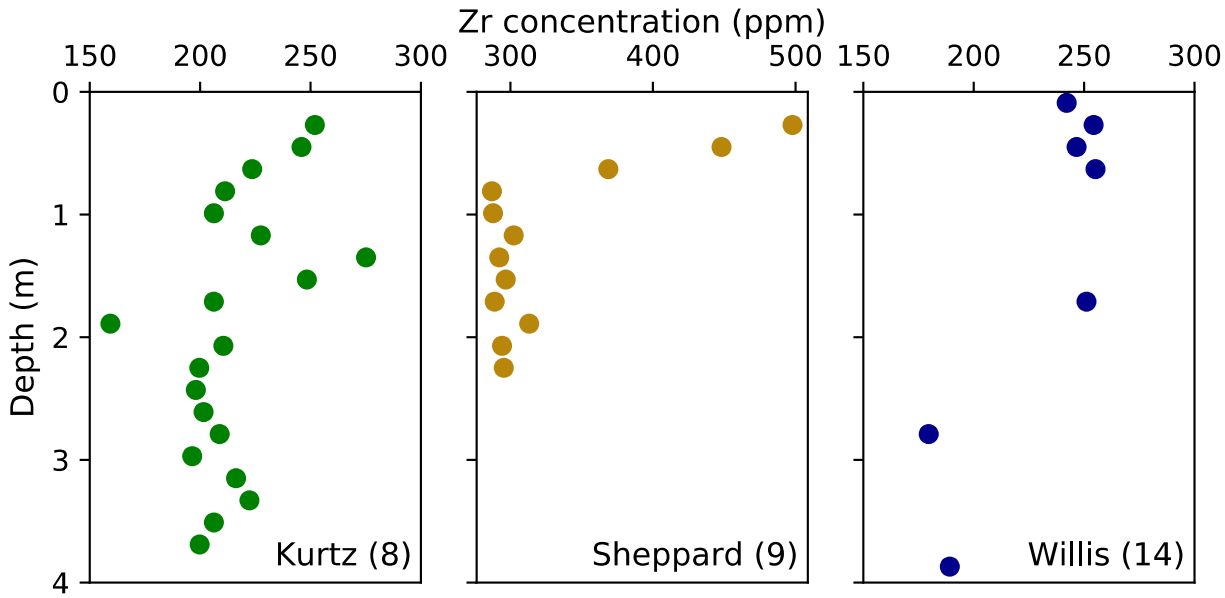

Figure S1. Zr concentrations versus depth at two sites last glaciated 16–19 ka (Kurtz and Willis) and a site we predict was last glaciated 868 ka (Sheppard).

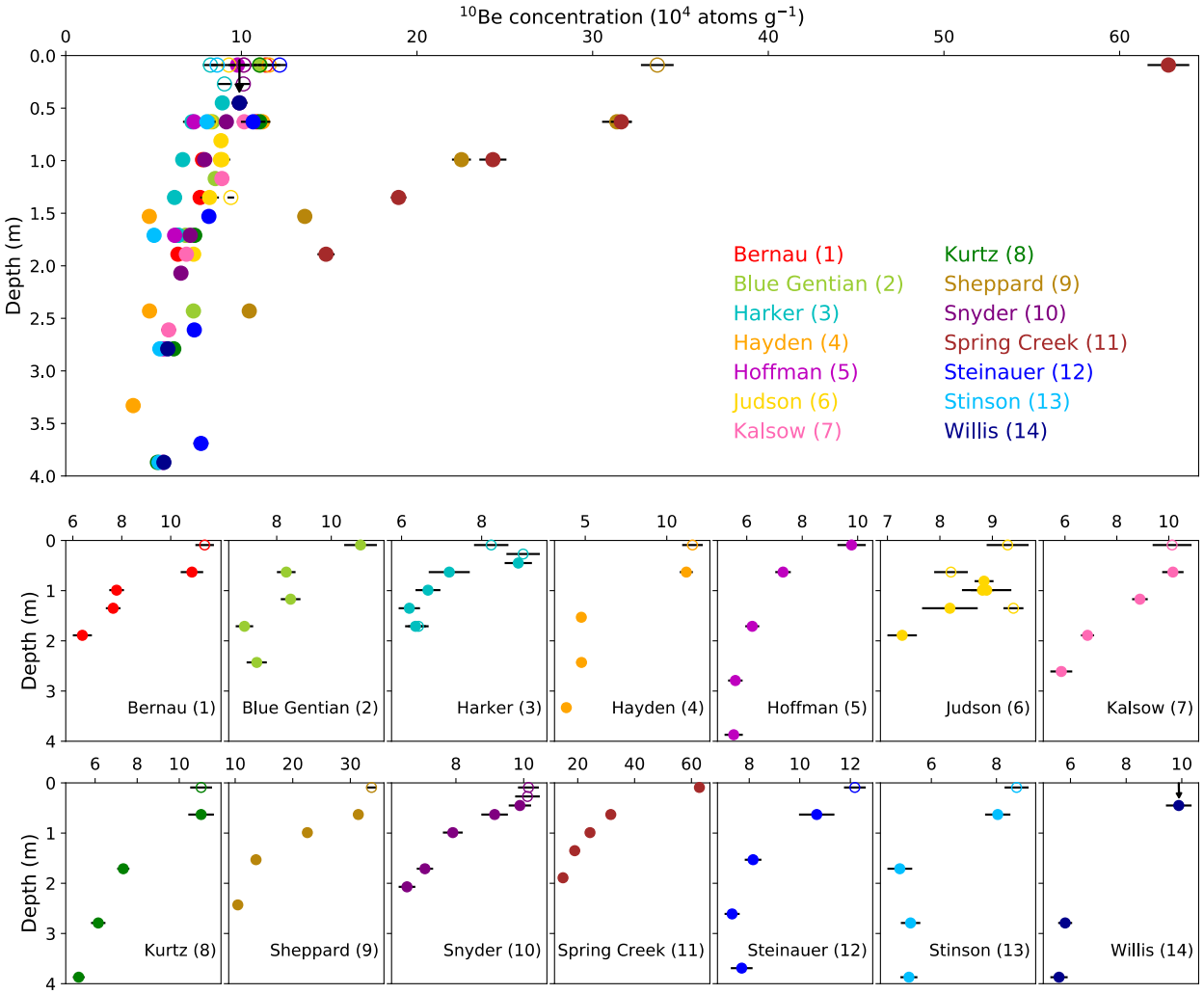

Figure S2. ^{10}Be depth profile results. Samples shown with open circles were not used in the depth profile fitting, generally because they fall withing the mixing zone near the ground surface.

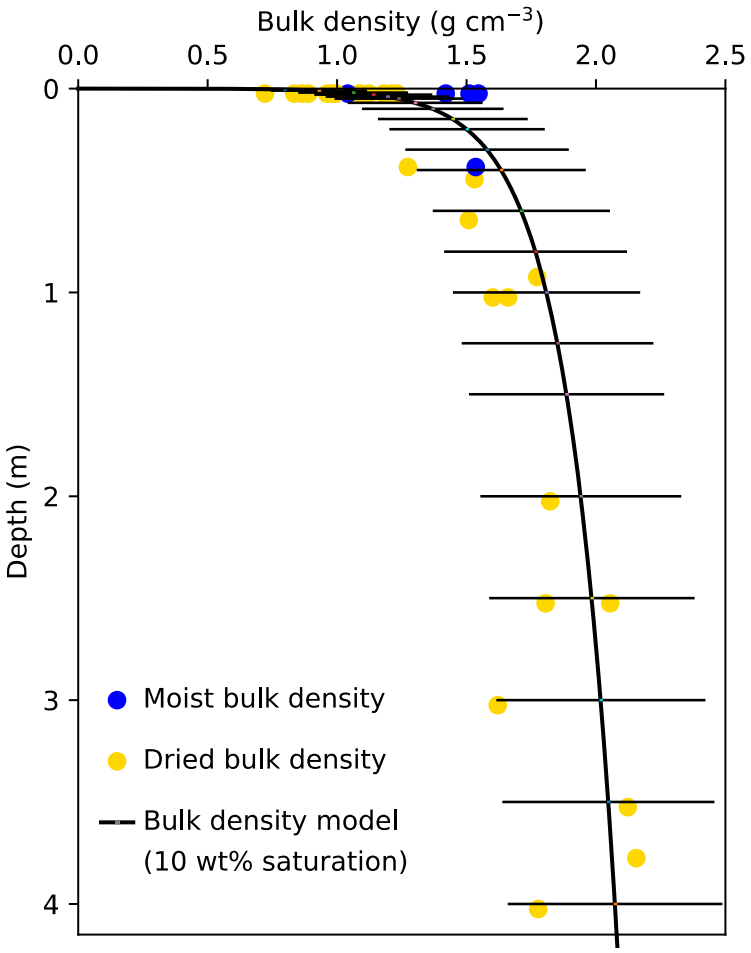

Figure S3. Bulk density model and sample measurements. The model assumes 10 percent by weight water content and is given by the function $\rho = 0.1909 \ln(z) + 0.9298 \pm 20\%$, where ρ = bulk density (g cm^{-3}) and z = depth (cm). The horizontal bars represent 20% uncertainty in the density value and were selected to conservatively span the measured values.